Highlights of Microwave Solar Research with Large Sidereal Arrays

M. R. Kundu

No Discussion of solar radio research done with

- single Dish Sidereal Telescopes
- Dedicated Solar Arrays
- Sidereal Arrays at meter & dkm & millimeter

(OVRO, CLRO, Nançay, Nobeyama, Toyokawa, Nagoya etc.)

Primary Instruments for Discussion

WSRT
VLA

Highlights of Microwave Solar Research with Large Sidereal Arrays

M. R. KUNDU
Univ. of MD.

1. Active Region studies ?
2. Preflare Active region studies ✓
3. Flare studies ✓
4. Quiet sun studies X

Observation	Results
June 9, 1973 3-el. interferometer X-ray & EUV data $\lambda = 3.7, 11.1$ cm 3", 9", 12 hr. resolution	First direct confirmation of gyro-resonance absorption theory. Near equality of radio T_b and X-ray-EUV determined T_e. Free-free absorption small, g-r absorption large, magnetic scale height $\sim 10^9$ cm - size of X-ray loop; magnetic field strength 300 Gauss. Kundu, Schmahl, Gerassimenko, Astron. Astrophys., 82, 265, 1980.
May 8-10 1974 WSRT $\lambda = 6$ cm 6", 10 sec. resolution	Confirmed general characteristics of old g-r model of SVC: close correspondence between brightest radio peaks and sunspots; radio emission associated with structures in which the field is nearly transverse (strong angle dependence of g-r process). Strong circular polarization (>50%) above sunspot and plage peaks. Radio maps (intensity and circular polarization) can be used as coronal magnetograms. Typical fields $\sim$ 600 Gauss. Kundu and Alissandrakis, Nature 257, 465, 1975. Kundu, Alissandrakis, Bregman and Hin, Ap.J., 213, 278, 1977.
July 1, 1979 WSRT $\lambda = 21$ cm 20" resolution 10 sec.	21 cm active regions consist of broad components, well resolved by WSRT. $T_b \sim 1 - 2 \times 10^6$ K. Peaks not correlated with sunspots. Absence of core-halo structure, unlike that observed at 2.8-6 cm; thermal emission. Bregman and Felli, Astron. Astrophys. 46, 41, 1976 Chiuderi-Drago, Felli and Tolfani, Astron. Astrophys., 61, 79, 1977.

Observation	Results
May 22-27, 1980 WSRT $\lambda = 6$ cm 3" resolution 10 sec	Detection of ring structure at 6 cm in sunspot-associated sources, with size between that of umbra and penumbra. Strongest emission peaks are weakly polarized, prominent V-peaks occur at the edges of strong sources. Interpreted as due to low g-r opacity at spot center and/or cool material above sunspots. Alissandrakis and Kundu, Ap.J., 253, L49, 1982 Strong, Alissandrakis, Kundu, Ap.J., 277, 865, 1984.
June 14, 16, 1981 WSRT $\lambda = 6$ cm 3" resolution	Similar to above; circularly polarized ($\sim$ 95%) horse-shoe structure associated with sunspot penumbra. Enhanced brightness temperature ($T_b \sim 10^6$) above umbra. Lang, and Willson, Ap.J., 255, L111, 1982.
Sept. 17, 1988 VLA $\lambda = 2$ cm 4" resolution 3 sec	Detection of g-r emission at coronal temperatures at 2 cm, implying that coronal field strengths can exceed 1800 Gauss, strong fields occur in a small source radiating in x-mode over penumbra of a large symmetric sunspot. Optically thin o-mode emission has peak $T_b \sim$ 36000 K and a hole over the umbra, consistent with expected low density material there. Appearance and location of x-mode source imply that strongest magnetic fields in the corona are localized in a compact flux tube. White, Kundu, Gopalswamy, Ap.J. Letters (in press), 1990.

Observation	Results
May 5, 1979 VLA $\lambda = 6$ cm 3.5" resolution	First detection of a stationary loop-like structure connecting two sunspots of opposite polarity in an active region. T_b at loop top 10^6 K and at foopoints $\sim 5 \times 10^6$ K. Low T_b in loop was attributed to optically thin thermal bremsstrahlung, and emission at foot points to gyroresonance process. Compact highly circularly polarized emission peaks were observed over some emerging flux regions, associated with arch filament systems (AFS). This association suggests that 6 cm emission may be related to neutral current sheets that might be generated above AFS in emerging flux regions. Kundu and Velusamy, Ap.J., 240, L63, 1980
May 16-19, 1981 VLA $\lambda = 20$ cm, June 15-16, 1981 VLA $\lambda = 20$ cm,	X-ray-like coronal loops observed at 20 cm. These loops have been interpreted as due to thermal bremsstrahlung as well to g-r process. Lang, Willson, & Rayole, Ap.J., 258, 384, 1982 McConnell and Kundu, Ap.J., 269, 698, 1983.
Jan. 28-29, 1984 VLA $\lambda = 17.4 - 21.8$ cm 4" resolution	Detection of cyclotron line by observing an active region at 10 closely spaced frequencies between 1440 and 1720 MHz; Willson found that T_b increased by a factor of $\sim$ 2.5 over the range of $\sim$300 MHz. The steep increase in T_b was interpreted as due to existence of neutral current sheets in a coronal loop where T and/or N are higher than in their surroundings. Willson's data re-analyzed by Zheleznyakov and Zlotnik who showed that the cyclotron line was probably produced at the third harmonic and not at the 4th or 5th harmonic as assumed by Willson. Willson, R. Ap.J., 298, 911, 1985 Zheleznyakov and Zlotnik, Soviet Astron. Letters, 14, 1957, 1988.

Preflare Active Region Studies

Observations	Results
June 25, 1980 VLA $\lambda = 6$ cm 2", 15 min resolution May 14, 1980 $\lambda = 6$ cm 3", 5 min resolution May 1, 1983 $\lambda = 2$ cm 2", 1 min. resolution	In general the active region emission increases in intensity and polarization over a period of several tens of minutes prior to the onset of a flare in that region. However, this phenomenon by itself does not appear to be sufficient to trigger a flare. A few minutes (< 10 min) just before the flare onset something else happens, usually in the form of (1) sudden change of polarization of the flaring regions; or (2) change of orientation of the neutral plane separating one polarity from another in a bipolar region; or (3) appearance of new sources in the immediate vicinity of some pre-existing structure of the active region. All three features are consistent with the emergence of new flux, which interacts with a pre-existing region to form a neutral or current sheet. The formation of the latter is ultimately responsible for triggering the onset of a flare. Kundu, Proc. SMY Int. workshop, Simferopol, p.24, 1981. Kundu, Schmahl, Velusamy, Vlahos, Astron. Astrophys., 108, 188, 1982. Velusamy and Kundu, Ap.J., 258, 388, 1982 Kundu and Shevgaonkar, Ap.J., 291, 860, 1985.

Observations	Results
May 8-10, 1974 WSRT $\lambda = 6$ cm 6", 30 sec. resolution	First 1-D fan beam observations showed that bursts (1-10 sfu) quite often occur near the neutral line of the coronal magnetic field, as determined from 2-D intensity and polarization maps. This observation suggests that energy release in flare occurs near the top of a loop. At impulsive phase burst source is compact (< 10"), strongly polarized, $T_b > 10^8$ K; in post-burst phase, it expands to > 1', unpolarized, $T_b \sim 10^6 K$.(1)
VLA $\lambda = 2, 1.3$ cm 1", 10 sec. resolution	First 2-D observation of a burst, showing that its source was located between Hα kernels, close to the magnetic neutral line. Burst source was compact (~ 2") in impulsive phase, and expands in the direction of orientation of the magnetic field lines joining the Hα kernels. Flare energy release was interpreted to be at the top of a loop; $T_B \sim 10^8 - 10^9$ K.(2)
June 25, 1980 VLA $\lambda = 6$ cm 1" × 2", 10 sec. resolution	Instead of a single loop, an arcade of loops may be involved at 6 cm in the flare process. The burst source has the same finite extent in both total intensity and polarization (5" × 10"); the neutral line passes thru the peak of total intensity and divides it into two regions of opposite polarity across the shorter extent of the region. This clearly implies an arcade of flaring loops in which the $\mu - \lambda$ burst is located near the top of the loop and occupies a significant portion of the legs of the loop. Hα occurs near the footpoints of the coronal loops; $T_B \sim 10^8 - 10^9$ K(3). 1. Alissandrakis and Kundu, Ap.J., 222, 342, 1978 2. Marsh and Hurford, Ap.J., 240, L111, 1980 3. Kundu, Schmahl, Velusamy, Ap.J., 253, 963, 1982.

Observations	Results
Theoretical Work	It is clear that the loop or arcade model of flares involves the release of energy in the coronal part of a magnetic loop. This energy release (possibly through magnetic reconnection brought on by a tearing mode instability: Spicer 1977) impulsively heats the plasma in the upper part of the loop. A non-thermal tail of high-energy electrons (energies up to a few hundred keV) may also be produced at this time. The hot plasma is confined between a pair of conduction fronts which propagate down the legs of the loop with a velocity near the ion sound speed (Brown et al 1979, Vlahos and Papadopoulos 1979). Electrons with velocities greater than approximately three times the electron thermal speed in this region, however, are not confined by the conduction fronts and escape to the lower part of the loop. Holman et al (1982) showed that, when the electron gyrofrequency exceeds the plasma frequency, the escaping electrons are unstable to the generation of electostatic plasma waves which scatter the particles in pitch angle to a nearly isotropic distribution. They showed that this scattering can enhance the microwave emission from the upper part of the loop, and the scattered electrons have a higher mean pitch angle. Petrosian (1982), on the other hand, computed the variation of gyrosynchrotron intensity and spectrum along a closed (semi-circular) magnetic loop. Using an isotropic particle distribution and a uniform (little variation from top to footpoints) magnetic field, he showed that microwave emission originated predominantly from the upper part of the loop and that a loop would appear larger in the optically thick regime than in the optically thin regime. Holman, Kundu and Papadopoulos, Ap.J., 257, 354, 1982. Petrosian, V., Ap.J., 255, L85, 1982.

Observations	Results
Nov. 13, 1981 VLA $\lambda = 6$ cm 2" × 1.5", 5" × 3", 12" resolution	Simultaneous observations at 2 and 6 cm wavelengths. The 6 cm burst source is located close to a magnetic neutral line, presumably near the top of a flaring loop, while the 2 cm emission originates from the footpoints of the loop. The 6 cm emission is dominated by gyrosynchrotron radiation of the thermal electrons in the bulk heated plasma at a temperature of $\sim 4 \times 10^7$ K, while the 2 cm emission is due to nonthermal particles released and accelerated during the flare process. From the observed low degree of polarization and the lack of the 2 cm source cospatiality with the 6 cm source a magnetic field of 200-300 G and $\delta > 4$ are estimated in the flare energy release site. A DC electric field flare model is invoked to explain the long delay between the peaks at the two wavelengths. From the delay, the strength of the electric field is estimated to be 0.2-4 μ statvolt cm^{-1} in the flaring region. Shevgaonkar and Kundu, Ap.J., 292, 733, 1985.
May 19, 1979 VLA $\lambda = 20$ cm 12" resolution	First spatially resolved observations of 20 cm radio emission originating from postflare loop systems. A 20 cm burst was associated with an Hα flare and a soft X-ray burst, and most of the intense radio emission occured at the end of the Hα flare and in the decay phase of the X-ray burst. The radio emission occurred in structures that are similar in size and shape to the systems of loops observed in X-rays. This postflare radio emission is similar to the Hα and X-ray emissions originating in postflare loops. The radio observations of postflare loops have the unique advantage that they offer an important means of determining the average magnetic field strength in these loops. Interpreting the radio emission in this particular event as thermal gyroradiation or as nonthermal synchrotron radiation, we estimate that the magnetic field strength lies in the range 120-170 gauss. Schmahl et al., Solar Phys., 83, 3, 1983.

Observations	Results
Nov. 5, 1980 VLA & SMM-HXIS $\lambda = 2$ cm, 16-30 KeV, 2" resolution	Microwave source at loop top and hard X-ray source at loop footpoints. Hoyng, Marsh, Zirin, Dennis, Ap.J., 268, 865, 1983.
VLA, WSRT NAG NOBE SMM HINOTORI $\lambda = 0.8$ - 20 cm 1"-20" resolution	Simultaneous microwave and hard X-ray imaging observations of 12 bursts show that it is difficult to discern a general pattern between microwave and hard X-ray burst locations. In général, the microwave source is displaced from the hard X-ray source. The commonly believed behavior of the microwave source being located near the top and hard X-ray source near the footponts of a loop appears to be true in some cases but not all. If the burst source is simple, both may be located near loop tops. Sometimes when the hard X-ray source has two components, one weak and one strong, the microwave source is not located over a neutral line (loop top) but close to a sunspot where the magnetic field is strongest. It appears that more than one loop or arcade may sometimes be involved in the microwave and hard X-ray emission. This is particularly true when several interacting loops trigger the onset of a flare. Kundu, M., Adv. Sp. Res., 4, 157, 1984 Takakura, Kundu, McConnell and Ohki, Ap.J., 298, 431, 1985.

Observations	Results
May 14, 1980 VLA $\lambda = 6$ cm 2", 10 sec. resolution	Evidence of magnetic reconnection in microwave flares. A preflare region with $T_b \sim 13 \times 10^6 K, p \sim 65\%$ existed before, extended along a neutral line in E-W direction. A gradual burst with $T_b \sim 40 \times 10^6$ and p $\sim$ 65-80% appeared at essentially same location. Intense emission ($T_b \sim 1.4 \times 10^8 K, p \sim 60\%$) extending along N-S neutral line (line of zero polarization at 6 cm), possibly due to reconnection. This north-south neutral line must be indicative of the appearance of a new system loops. In the 20 sec preceding the impulsive peak ($T_b \sim 1.1 \times 10^8 K; p \sim 40\%$) the arcade of loops (burst source) changed and ultimately developed into two strong bipolar regions or a quadrupole structure whose orientations were such that near the loop tops the field lines were opposed to each other. This quadrupole field configuration is reminiscent of the flare models in which a current sheet develops at the interface between two closed loops. The impulsive energy release must have occured due to magnetic reconnection of the field lines connecting the two oppositely polarized bipolar regions. After the impulsive phase was over, the gradual burst still continued for another 10 min, with the magnetic field configuration being very similar to what existed in the gradual phase prior to the impulsive event.
June 24, 1980 VLA $\lambda = 6$ cm 18", 10 sec. resolution	Interacting loops before onset of impulsive flare associated with a hard x-ray burst. Kundu, Schmahl, Velusamy, Vlahos, Astron. Astrophys., 108, 188, 1982. Velusamy and Kundu, Ap.J., 258, 388, 1982. Kundu, Machado, Erskine, Rovira and Schmahl, Astron. Astrophys., 132, 241, 1984.

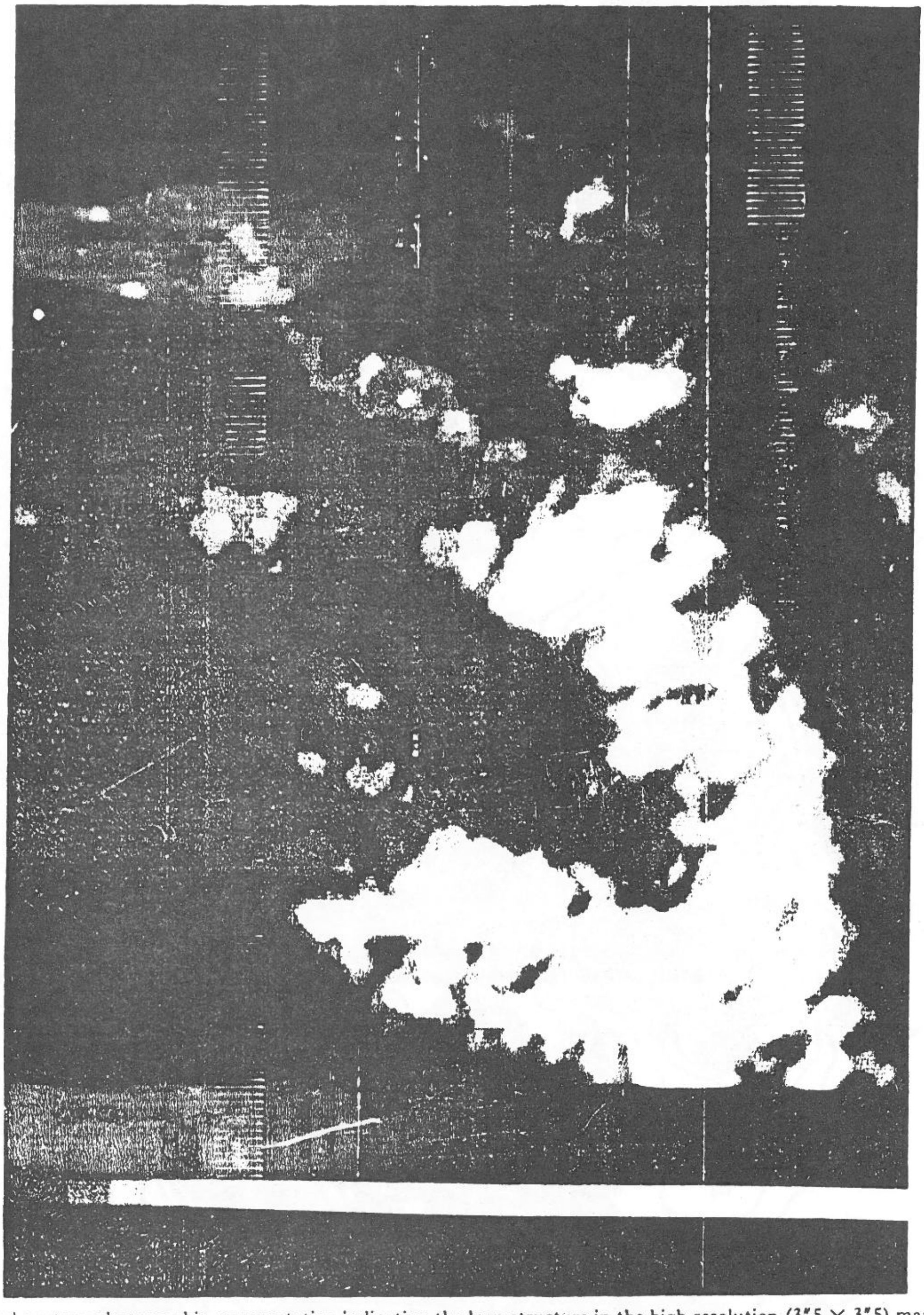

FIG. 4.—Shaded contour photographic representation indicating the loop structure in the high-resolution (3".5 × 3".5) map of the right-circularly polarized intensity. The intensity scale is shown at the bottom of the photograph.

KUNDU AND VELUSAMY (*see* page L64)

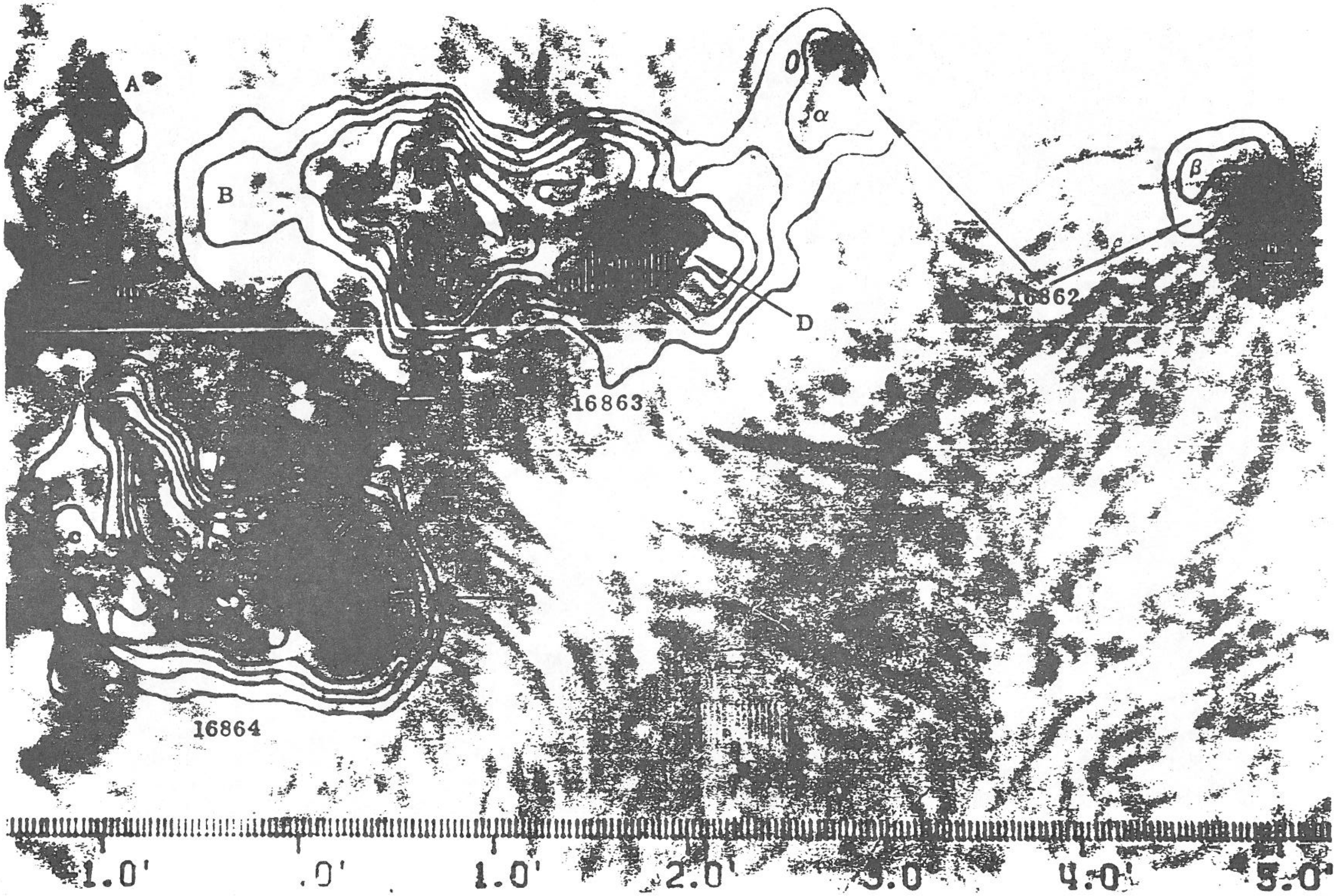

FIG. 1*a*

FIG. 1.—Total intensity (*a*) and circular polarization (*b*) contours for 1980 May 25 at 6 16 cm overlaid on an Hα photograph obtained from the observatory at Athens. Three active regions are included in the field of view. The contours are in steps of 5 × 10[illegible] K for the total intensity and 1.5 × 10^5 K for the circular polarization. Hatched contours show decreasing brightness temperature. The scale is in minutes of arc.

ALISSANDRAKIS AND KUNDU (see page L49)

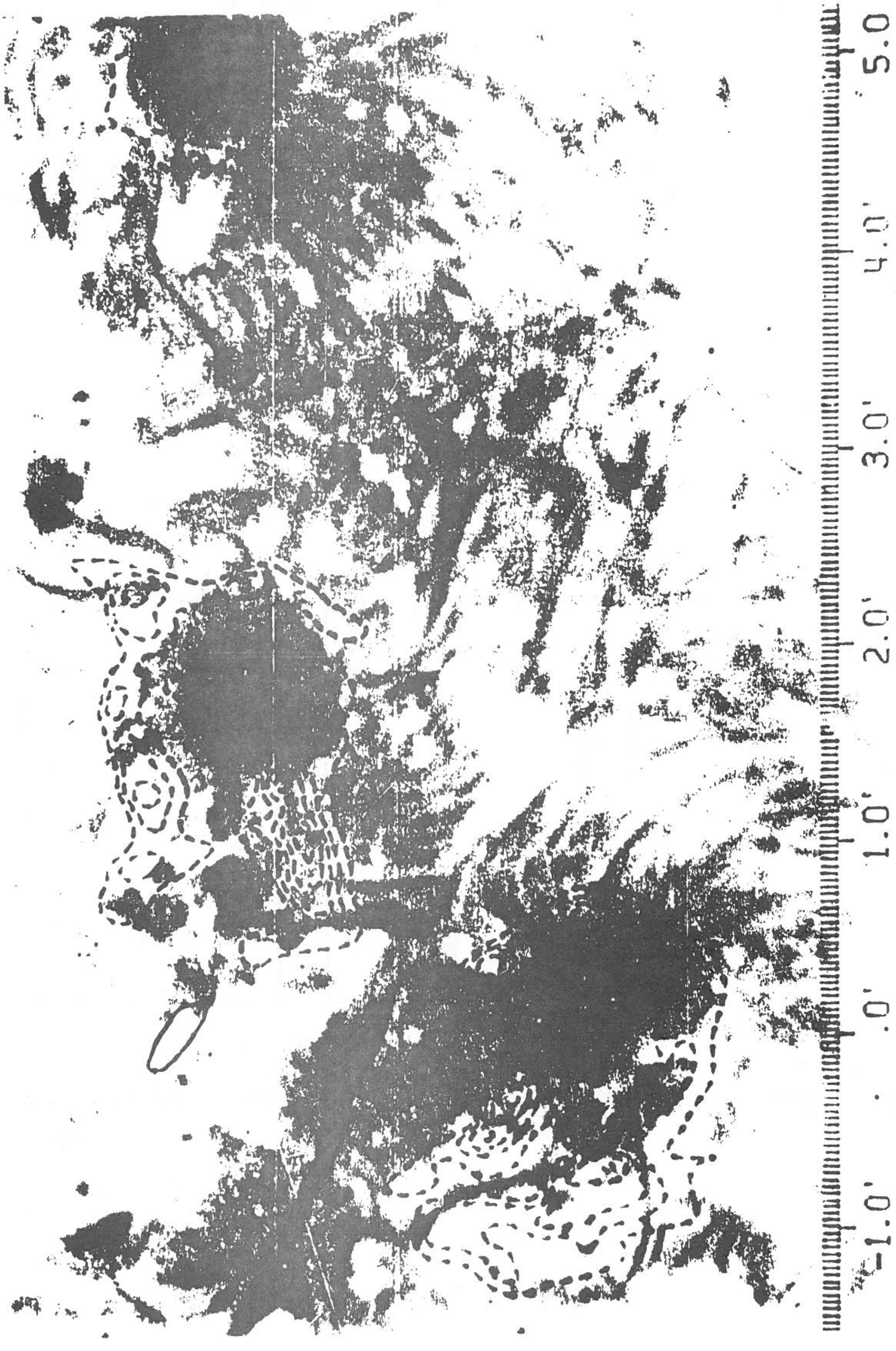

Fig. 1b

Alissandrakis and Kundu (*see* page L51)

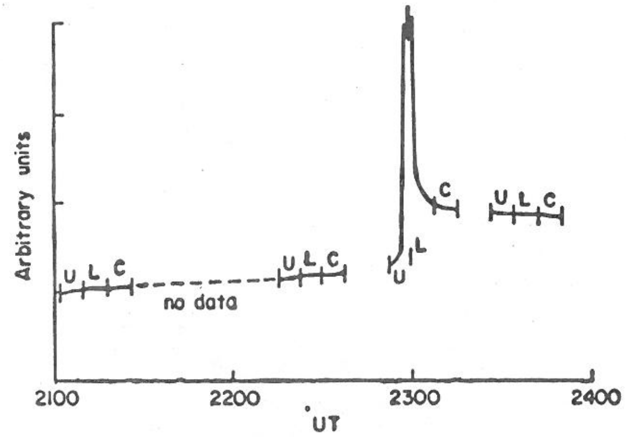

FIG. 1.—Flux vs. time profile of the burst in arbitrary units. Blocks denoted by *L*, *C*, and *U* represent the time intervals during which 20, 6, and 2 cm observations, respectively, were taken.

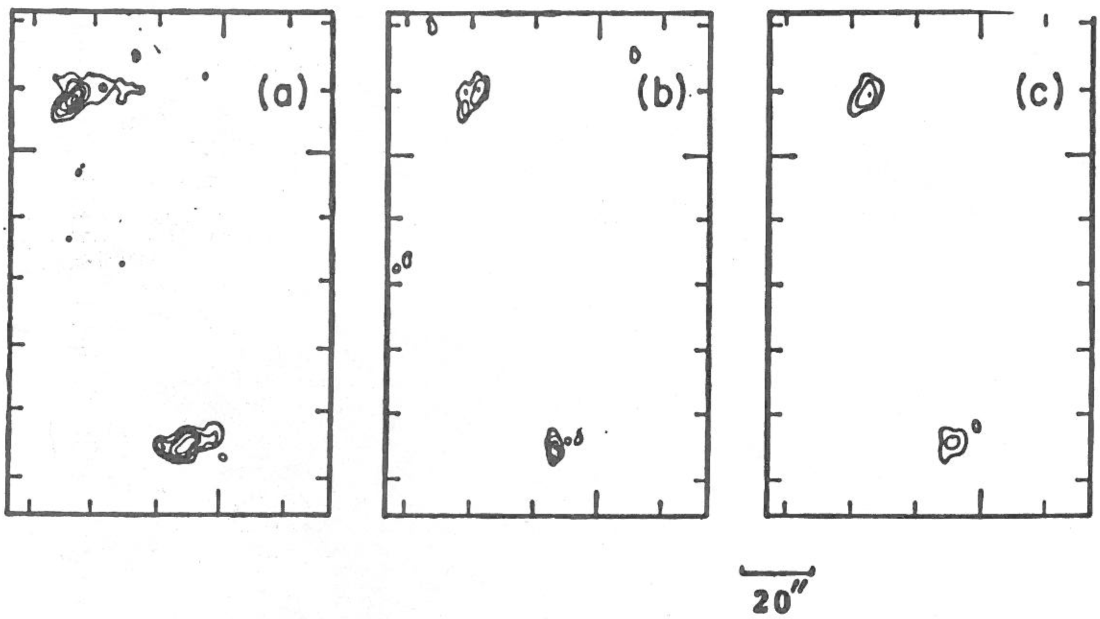

FIG. 2.—(*a*) Twelve hour synthesized total intensity (*I*) map of the active region at 2 cm; contour interval is 2.9×10^4 K. (*b*) *I*-map during 21:02–21:10 UT; contou[illegible] nterval is 1.9×10^5 K. (*c*) *I*-map during 22:15–22:22 UT; contour interval is 1.9×10^5 K.

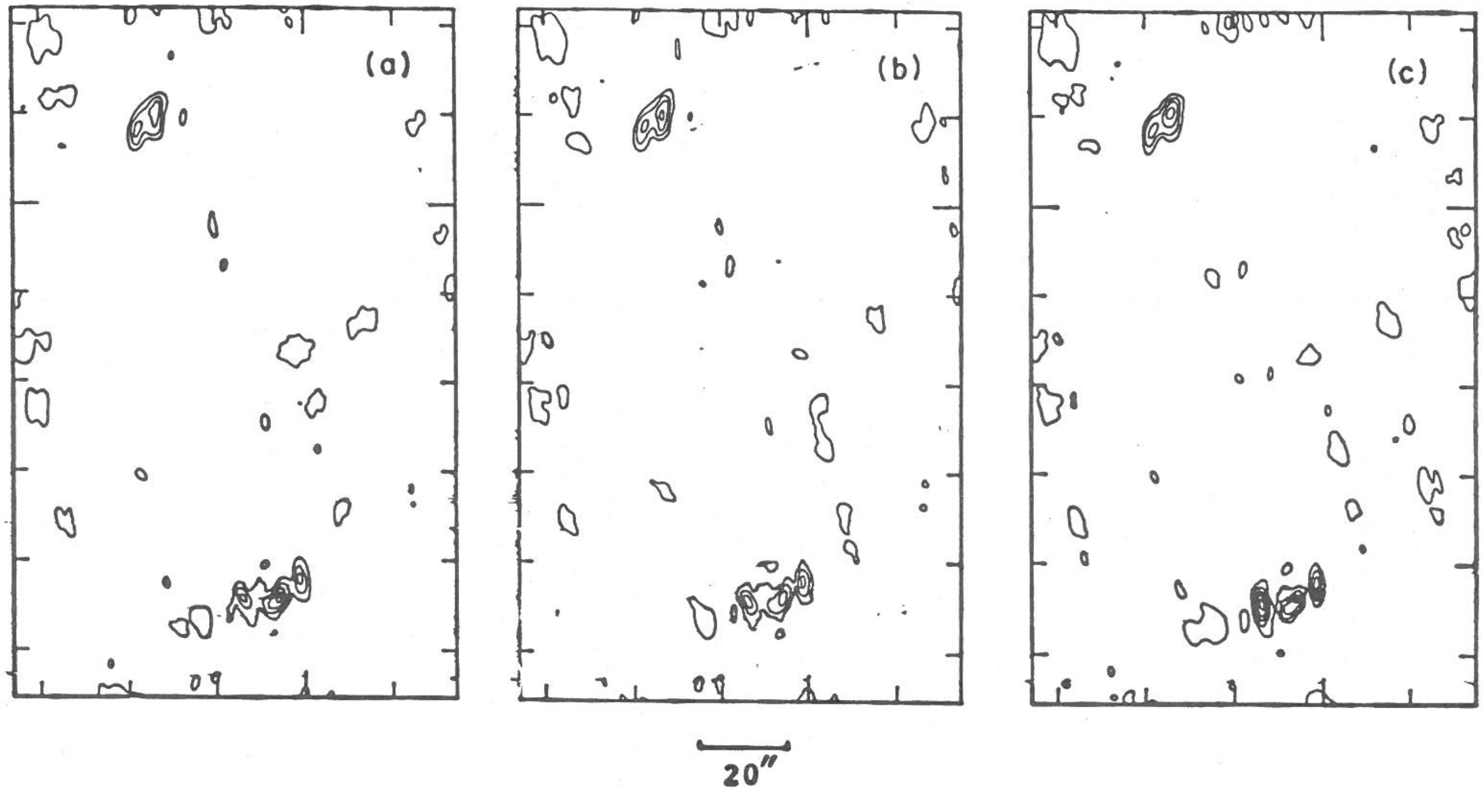

FIG. 3.—(a, b) One minute maps at 2 cm just before the onset of the flare; (c) 1-minute map at 2 cm at the beginning of the impulsive phase. Contour interval is 1.9×10^5 K.

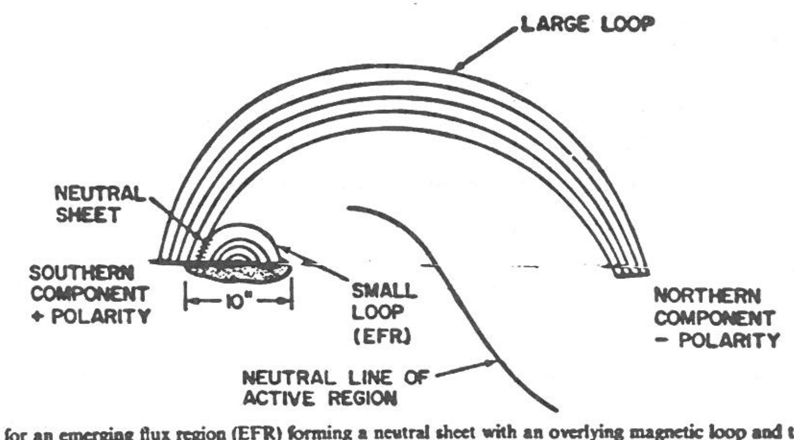

FIG. 5.—A schematic model for an emerging flux region (EFR) forming a neutral sheet with an overlying magnetic loop and triggering the onset of a flare. A similar schematic model was produced by Kahler, Petrasso, and Kane (1976).

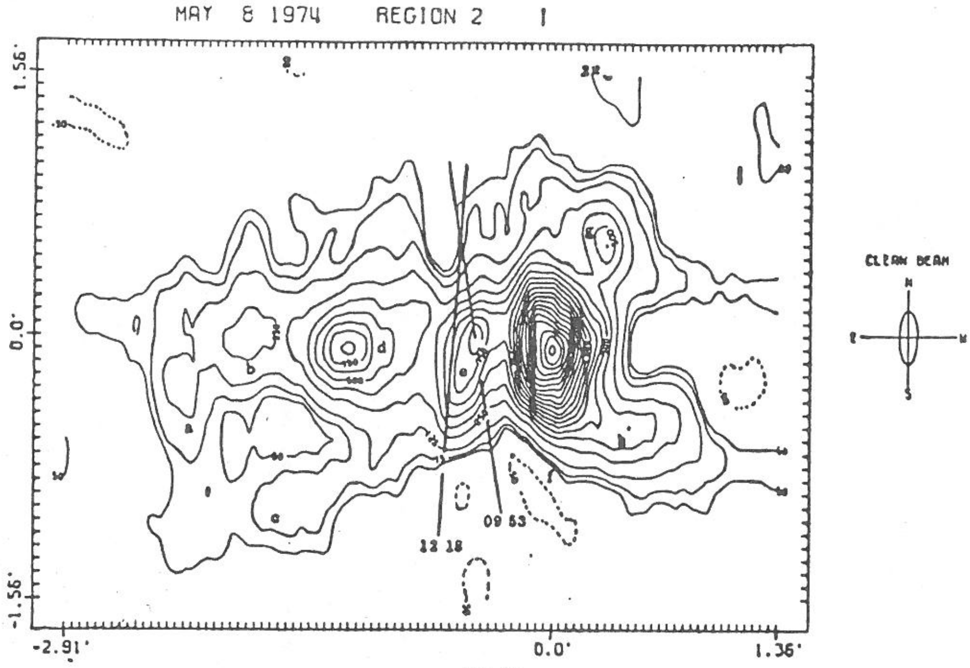

FIG. 4a

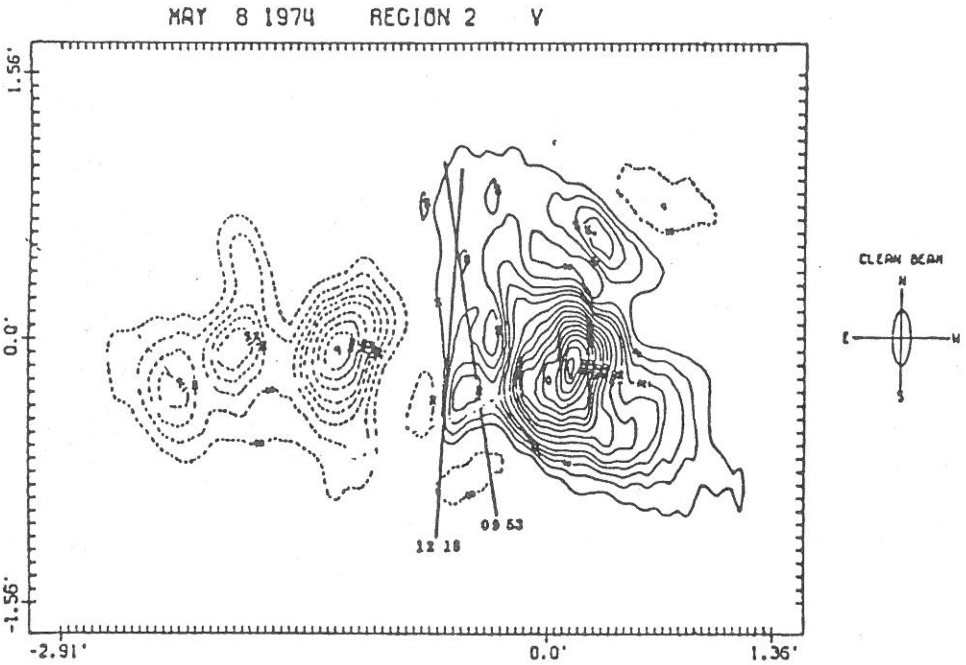

FIG. 4b

FIG. 4.—Total intensity (I) and circular polarization (V) maps of region 2 for May 8, 9, and 10. The contour labels are in thousands of degrees K above the solar background. Dashed lines indicate negative values; positive V values correspond to right circularly polarized radiation. The straight lines show the loci of possible positions of bursts, marked with the UT at maximum. The contour levels are: May 8 and May 9, I: 50, 75, 125, 250, etc. May 8, V: ±30, ±60, ±90, etc. May 9, V: ±7.5, ±15, ±30, −60, etc. May 10, I: 25, 50, 75, 250, etc. May 10, V: ±4, ±8, −15, −30, −60, etc. ($\times 10^3$ K).

M.R. Kundu

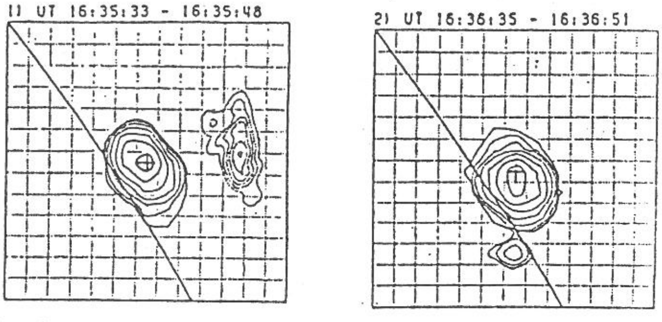

Fig. 3. HINOTORI-SXT hard X-ray images (20–30 Kev) and VLA 6 cm images are indicated by solid and dashed contours respectively for a limb flare that occurred on August 3, 1981. The X-ray images were produced at 16:35 and 16:37 UT. The solid curve is the west limb /13/.